

Received August 16, 2019; reviewed; accepted September 26, 2019

## Interaction of sulfuric acid with dolomite (104) surface and its impact on the adsorption of oleate anion: a DFT study

Qinbo Cao <sup>1,2</sup>, Heng Zou <sup>1</sup>, Xiumin Chen <sup>1,2</sup>, Xingcai Yu <sup>2</sup>

<sup>1</sup> Faculty of Land Resources Engineering, Kunming University of Science and Technology, Kunming 650093, Yunnan, PR China

<sup>2</sup> State Key Laboratory of Complex Nonferrous Metal Resources Clean Utilization, Kunming 650093

Corresponding authors: cabdxx@163.com (Qinbo Cao), chenxiumin9@hotmail.com (Xiumin Chen)

**Abstract:** Sulfuric acid (H<sub>2</sub>SO<sub>4</sub>) is a specific depressor for apatite rather than for dolomite. The H<sub>2</sub>SO<sub>4</sub>-treated dolomite can still be floated effectively by oleate. However, the role of H<sub>2</sub>SO<sub>4</sub> in the adsorption of oleate onto dolomite surface remains unclear. In this work, density functional theory calculations were conducted to probe the interactions among sulfate anion (SO<sub>4</sub><sup>2-</sup>), oleate anion and the dolomite surface. The adsorption behaviors of SO<sub>4</sub><sup>2-</sup> anion onto the perfect and CO<sub>3</sub>-defect dolomite surfaces were compared. Such results show that SO<sub>4</sub><sup>2-</sup> anion could only adsorb onto the defective dolomite surface, where it bonded with a Ca atom. The remaining Ca and Mg atoms at the defect site could further react with the oleate anion, generating new Ca/Mg-O ionic bond. In this regard, oleate and SO<sub>4</sub><sup>2-</sup> anions may both present on the dolomite surface. This phenomenon accounts for the flotation of H<sub>2</sub>SO<sub>4</sub>-treated dolomite.

**Keywords:** dolomite, adsorption, oleate, depressor, density functional theory

### 1. Introduction

Flotation is a primary method for enriching apatite from its deposits (Matis and Zouboulis, 2001). Flotation techniques depend on the efficient adsorption of a collector onto the target mineral surface to generate a hydrophobic surface (Temel, 2015). Considerable effort has been devoted to improving the adsorption capacity of collectors on the apatite surface (Peres et al., 2005).

Currently, with the depletion of high-grade apatite ores, low-grade ores with a large amount of Ca-bearing gangue minerals, such as dolomite, are becoming important phosphate resources in China (Ruan et al., 2019). The separation of apatite from other Ca-bearing minerals is attracting intensive interest, because this issue determines the success of apatite flotation to a certain extent. Fatty acids, such as oleate, are widely used as collectors for apatite flotation (Horta et al., 2016). However, these collectors exhibit poor selectivity for the flotation of Ca-bearing minerals. Thus, depressors or more selective collectors are required for the flotation separation of apatite from other Ca-bearing gangue minerals.  $\beta$ -naphthyl sulfonate formaldehyde condensate can be used as a selective depressor for dolomite (Yu et al., 2016). Liquid glass, citric acid and sodium pyrophosphate also showed depressing effects on calcite flotation (Chen et al., 2018; Kondrat'Ev et al., 2017). The mixture of hydroxamic acids and alcohol is a selective collector in phosphate flotation system (Wang et al., 2006). Several amino acid-based collectors can be used as selective collectors in the apatite-calcite flotation system (Karlkvist et al., 2015; Zou et al., 2019).

Phosphate flotation plants prefer using a reverse flotation method to separate apatite from dolomite (Liu et al., 2017a). In this method, sulfuric acid (H<sub>2</sub>SO<sub>4</sub>) is widely used as a specific depressor for apatite. However, this inorganic acid cannot prevent the flotation of dolomite with a fatty acid collector (Zou et al., 2019). In this regard, apatite and dolomite are well separated from each other in weak acid slurry. The depressing mechanism of H<sub>2</sub>SO<sub>4</sub> for apatite flotation is well understood. The adsorption of a fatty

acid collector onto apatite surface depends on the interaction between the collector and the Ca atoms on the apatite surface. As a result, the chemisorbed oleate or the surface precipitation of dioleate salt forms on the apatite surface (Lu et al., 1998). After treatment with  $\text{H}_2\text{SO}_4$ , calcium sulfate ( $\text{CaSO}_4$ ) species may form on the apatite surface due to the extremely low solubility of  $\text{CaSO}_4$  (Liu et al., 2017b). The  $K_{\text{sp}}$  of  $\text{CaSO}_4$  is  $9.1 \times 10^{-6}$ , and thus  $\text{CaSO}_4$  is a sparingly soluble salt (Xiaojun and Kelebek, 2000). The formed  $\text{CaSO}_4$  species on the apatite surface may hinder the adsorption of a collector at the Ca sites on the apatite surface.

In the case of dolomite, it is interesting to notice that oleate can still float the  $\text{H}_2\text{SO}_4$ -treated dolomite. Oleate can react with Ca and Mg atoms on the natural dolomite surface to achieve chemisorptions or form  $\text{Ca}(\text{OI})_2$  and  $\text{Mg}(\text{OI})_2$  precipitations (Mathur and Moudgil, 1994). In  $\text{H}_2\text{SO}_4$  solution, Ca atoms on the dolomite surface may also react with sulfate ( $\text{SO}_4^{2-}$ ) anion to form  $\text{CaSO}_4$  species. However, the solubility of magnesium sulfate ( $\text{MgSO}_4$ ) is 355g/L at 20 °C (Kushch et al., 2011). Due to the high solubility of magnesium sulfate ( $\text{MgSO}_4$ ),  $\text{MgSO}_4$  precipitation cannot occur on the dolomite surface. Therefore, researchers generally believe that oleate can still adsorb at the Mg site on the  $\text{H}_2\text{SO}_4$ -treated dolomite surface. However, no direct evidence has been provided to support this argument. In fact, oleate species and  $\text{SO}_4^{2-}$  can co-adsorb onto the  $\text{H}_2\text{SO}_4$ -treated dolomite surface (Zou et al., 2019). Furthermore,  $\text{Mg}(\text{OI})_2$  ( $K_{\text{sp}}=1.58 \times 10^{-14}$ ) and  $\text{Ca}(\text{OI})_2$  ( $K_{\text{sp}}=3.98 \times 10^{-16}$ ) may precipitate on the  $\text{H}_2\text{SO}_4$ -treated dolomite surface (Michaux et al., 2018; Zou et al., 2019); this observation disagrees with the common knowledge that oleate can only bind with Mg atoms on the  $\text{H}_2\text{SO}_4$ -treated dolomite surface. The adsorption sites of oleate on the  $\text{H}_2\text{SO}_4$ -treated dolomite are still not fully understood.

The surface features of dolomite in  $\text{H}_2\text{SO}_4$  solution is complex. Carboxyl anion ( $\text{CO}_3^{2-}$ ) on the dolomite surface may dissociate into  $\text{CO}_2$  and  $\text{H}_2\text{O}$  in the  $\text{H}_2\text{SO}_4$  solution (Chanturiya et al., 2011). As a result of the dissociation of the  $\text{CO}_3^{2-}$ , several Mg/Ca atoms on the dolomite surface may be exposed to the solution and further react with oleate. However, such assumption is difficult to be verified by experimental methods. By contrast, computer simulation is a reliable method for evaluating the adsorption behavior of a collector onto apatite and dolomite surfaces (Cao et al., 2019); it is a useful tool to design more efficient and selective collectors for phosphate flotation (Pradip and B, 2003; Pradip et al., 2002; Rai et al., 2008; Rai and Pradip, 2012). To date, density functional theory (DFT) calculation has been widely applied to assess the adsorption behavior of metal ions or surfactants on a mineral surface (Jiao et al., 2016; Sarvaramini et al., 2016). DFT is a method to solve the Schrodinger's equation, and it can be used to calculate the ground state of a system (Segall et al., 2002). DFT calculation can determine the adsorption energy and structure of a collector on a mineral surface, and the electronic structure properties of the adsorption structure. However, few researchers have used this method to address the interaction of oleate with the dolomite surface treated by  $\text{H}_2\text{SO}_4$ .

The current work aimed to further clarify the interactions among  $\text{H}_2\text{SO}_4$ , oleate and dolomite surface at the atomic level via DFT calculations. First, the binding behaviors of  $\text{SO}_4^{2-}$  anion on the perfect and  $\text{CO}_3$ -defect dolomite surfaces were compared to determine the possible reactions between  $\text{H}_2\text{SO}_4$  and dolomite surface. Furthermore, the adsorption of oleate onto the dolomite surface with the presence of  $\text{SO}_4^{2-}$  anion was investigated to elucidate the flotation mechanism of dolomite in  $\text{H}_2\text{SO}_4$  solution.

## 2. Theoretical calculations

The Cambridge Serial Total Energy Package (CASTEP) based on the density functional theory was used in all the calculations (Segall et al., 2002). The exchange-correlation functional was treated using generalized gradient approximation (GGA) with the Perdew-Burke-Ernzerhof (PBE) functional (Perdew et al., 1996; Perdew and Zunger, 1981). Electron-ion interactions were described on the basis of the ultrasoft pseudo-potential (Francis and Payne, 1990). Brillouin zone integrations were performed using a  $2 \times 2 \times 1$  k-point mesh, and the kinetic energy cutoff during the calculations was 400 eV. The accuracy of the energy convergence was  $1 \times 10^{-6}$  eV/atom and the maximum force and ionic displacement were 0.03 eV/Å and 0.001 Å, respectively. As tested, such parameters were sufficient to achieve a numerical convergence. A three-layer model of dolomite (104) surface with 35 Å of vacuum layer was used in this work, because the (104) surface is the cleavage plane of the dolomite (Kyllönen et al., 2004). This dolomite model is the same as the model used in (Cao et al., 2019).

The adsorption energy ( $\Delta E_{\text{ad}}$ ) of  $\text{SO}_4^{2-}$  or oleate anion on the dolomite surface was calculated using

the following equation:  $\Delta E_{ad} = E_{adsorbate+slab} - E_{adsorbate} - E_{slab}$ , where  $E_{slab}$  and  $E_{adsorbate}$  refer to the total energies of the dolomite (104) slab model and an adsorbate ( $\text{SO}_4^{2-}$  or oleate anion), respectively, before the interaction; and  $E_{adsorbate+slab}$  is the total energy of the dolomite surface with an adsorbate. The energies of  $\text{SO}_4^{2-}$  and oleate anions were calculated using the gamma point, and their formal charges were set as  $-2e$  and  $-1e$ , respectively.

### 3. Results and discussion

#### 3.1 Adsorption onto the perfect dolomite (104) surface

As stated in the Introduction,  $\text{SO}_4^{2-}$  is expected to bond with the dolomite surface. Here,  $\text{SO}_4^{2-}$  was placed on the perfect dolomite (104) surface at various initial sites, to determine the possible interaction structures. Consequently, four binding models were observed on the dolomite surface (Fig. 1). However, the adsorption energy of each binding structure was positive. Hence, the adsorption of  $\text{SO}_4^{2-}$  onto the perfect dolomite (104) surface is not an energetically favorable process. The first atomic layer of dolomite surface consisted of the O atoms of the carbonate groups. It seems that the electrostatic repulsion force between  $\text{CO}_3^{2-}$  and  $\text{SO}_4^{2-}$  anions may prevent the adsorption of  $\text{SO}_4^{2-}$ .

In fact, the  $\text{CO}_3^{2-}$  on the dolomite surface is unstable in an acidic solution as mentioned in the Introduction.  $\text{CO}_3^{2-}$  anion may dissociate into  $\text{H}_2\text{O}$  and  $\text{CO}_2$ , according to reaction 1 (" $\equiv$ " refers to the surface) (Chanturiya et al., 2011). Therefore, defect sites can be generated on the dolomite surface, where the electrostatic repulsion between  $\text{SO}_4^{2-}$  and the surface is reduced due to the absence of  $\text{CO}_3^{2-}$ . Consequently,  $\text{SO}_4^{2-}$  may bind to the Ca atom in a defect site (reaction 2). To examine this assumption, we further probed the adsorption of  $\text{SO}_4^{2-}$  onto the defective dolomite (104) surface.

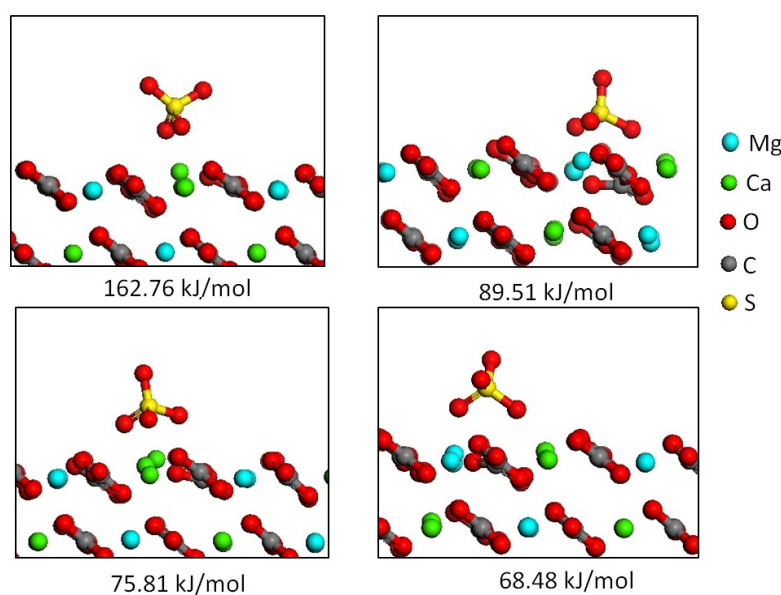
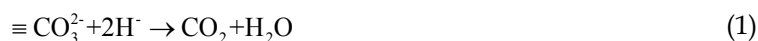


Fig. 1. Binding structures and energies of  $\text{SO}_4^{2-}$  anion on the perfect dolomite (104) surface

One  $\text{CO}_3^{2-}$  anion on the dolomite (104) surface was removed to generate the defect dolomite surface (Fig. 2). Several possible bonding metal atoms on this defective dolomite surface were also numbered, as shown in Fig. 2. It was found that  $\text{SO}_4^{2-}$  could interact with the Ca1 or Ca2 atom at the defect site (Fig. 3). The adsorption energies of  $\text{SO}_4^{2-}$  at the Ca1 and Ca2 sites were  $-356.20$  kJ/mol and  $-459.54$  kJ/mol, respectively. The length of the  $\text{O}_{(\text{sulfate})}$ -Ca bond ranged from  $2.16 \text{ \AA}$  to  $2.72 \text{ \AA}$ . These results indicate that  $\text{SO}_4^{2-}$  can readily interact with the Ca atoms on the defective dolomite surface.

On the basis of the DFT calculation results, the reaction of  $\text{H}_2\text{SO}_4$  with the dolomite surface could be delineated into the following steps: First, two  $\text{H}^+$  ions interacted with one  $\text{CO}_3^{2-}$  anion on the dolomite

surface, and dissociates the  $\text{CO}_3^{2-}$ . Thus, a defect site was formed on the dolomite surface; Further, a  $\text{SO}_4^{2-}$  anion reacted with a Ca atom at the defect site to achieve adsorption.

Theoretically, the number of defect sites on the dolomite surface may be equivalent to that of  $\text{SO}_4^{2-}$  generated from  $\text{H}_2\text{SO}_4$ . At each defect site, two Ca atoms allow the adsorption of  $\text{SO}_4^{2-}$ . However, a  $\text{SO}_4^{2-}$  anion can only react with a Ca atom at each defect site. In this regard, another Ca atom at the defect site remains to interact with oleate. This adsorption behavior may account for the formation of Ca-oleate species on the  $\text{H}_2\text{SO}_4$ -treated dolomite surface. The adsorption features of oleate on such defective surface with a  $\text{SO}_4^{2-}$  anion was further investigated in the following section.

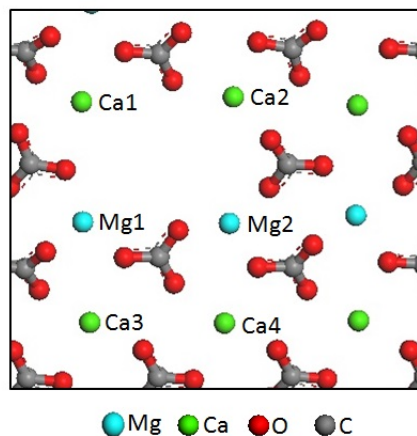


Fig. 2. Top view of the defective dolomite surface used in the DFT study (only atoms on the top of the surface are shown)

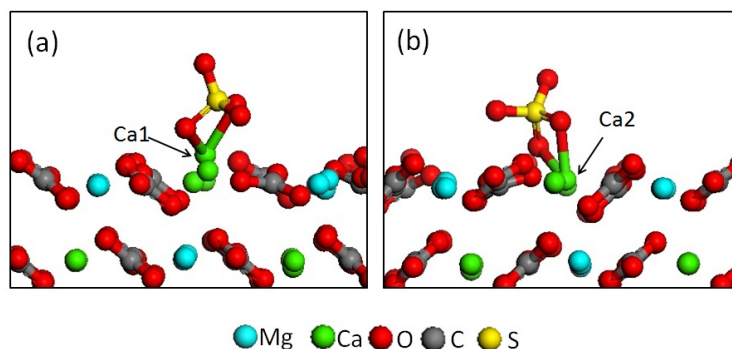


Fig. 3. Binding structures of  $\text{SO}_4^{2-}$  anion on the defective dolomite surface: (a) at the Ca1 site and (b) at the Ca2 site

### 3.2 Adsorption of oleate anion onto the $\text{H}_2\text{SO}_4$ -treated dolomite surface

Flotation using oleate as a collector is commonly performed in a weak basic solution, where oleate anion is the dominant species in the solution (Qinbo et al., 2017). By contrast, the reverse flotation of dolomite using  $\text{H}_2\text{SO}_4$  as a depressor is conducted in slightly acidic slurry, where the pH of the slurry is nearly 5. At this pH value, oleate anion is still the primary species to react with the dolomite surface, according to the previous FTIR results (Qinbo et al., 2017). Hence, the current work focused on the adsorption of oleate anion onto the dolomite surface. The stable geometry of oleate anion was first determined before probing the interaction between the collector and the dolomite surface. The structure of isomer of oleate anion, namely iso-oleate anion, was also calculated for comparison.

For the optimized oleate anion, a double bond existed between C9 and C10 atoms, and the bond angle of C10-C9-C8 was  $121.13^\circ$  (Fig. 4). In this regard, oleate anion exhibited a nonlinear structure. Whereas, the iso-oleate anion presented a linear structure. The double bond in iso-oleate did not result in the winding of the molecule. As calculated by the CASTEP code, the energy of oleate anion ( $-404892.65$  kJ/mol) was  $23.94$  kJ/mol lower than that of iso-oleate anion ( $-404937.58$  kJ/mol). Thus,

the structure of oleate is more favorable than that of iso-oleate. This result supports the fact that oleate is prevalent over iso-oleate in natural vegetable oils (Ariffin et al., 2009).

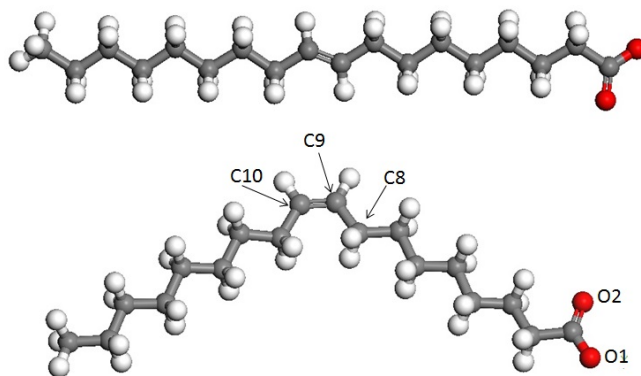


Fig. 4. Optimized structures of iso-oleate anion (top) anion and oleate anion (bottom). Three C atoms and two O atoms were numbered in the figure

Furthermore, the defective dolomite (104) surface with a  $\text{SO}_4^{2-}$  bonding to Ca2 was used to assess the interaction between the oleate anion and the mineral surface, because the adsorption of  $\text{SO}_4^{2-}$  anion at the Ca2 site was preferred over that at the Ca1 site.

It was observed that oleate anion could interact with the Ca atom and Mg atoms at the defect site of the dolomite surface to form three bidentate binding structures: Bi1, Bi2 and Bi4 structures (Fig. 5). Oleate anion could also react with two Mg atoms (Mg1 and Mg2) to produce a bidentate binding (Bi3) model. The two O atoms of oleate could coordinate with the Ca1 atom to generate a surface chelation complex. The adsorption energies of these binding structures were all negative (Table 1), which reveals that oleate anion could spontaneously bind to this type of dolomite surface. In terms of bond length results, the bond length of  $\text{O}_{(\text{oleate})}\text{-Mg}$  was slightly shorter than that of  $\text{O}_{(\text{oleate})}\text{-Ca}$ , probably because the ionic radius of Mg ion is relatively smaller.

Table 1. Binding energies (kJ/mol) and bond lengths (Å) of oleate anion on the defective dolomite surface with a  $\text{SO}_4^{2-}$  anion initially bonding with Ca2

Models	$\Delta E_{ad}$	Bond length	
Bi1	-246.62	O2-Ca1 (2.15)	O1-Mg1 (1.91)
Bi2	-207.45	O1-Ca4 (2.27)	O2-Mg2 (1.92)
Chelation	-133.59	O1-Ca1 (2.16)	O2-Ca1 (2.35)
Bi3	-72.53	O2-Mg2 (2.03)	O1-Mg1 (1.99)
Bi4	-66.45	O2-Mg1 (1.95)	O1-Ca3 (2.43)

On the other hand, the adsorption of oleate on the dolomite surface could alter the location of  $\text{SO}_4^{2-}$  on the surface (Fig. 6). For the B1 and chelation models,  $\text{SO}_4^{2-}$  anion migrated to the bridge site of Ca2 and Mg2 due to the adsorption of oleate anion. For the Bi2 model,  $\text{SO}_4^{2-}$  moved to the bridge site between Ca1 and Ca2. Although the positions of  $\text{SO}_4^{2-}$  changed in these models, the  $\text{SO}_4^{2-}$  was still adsorbed onto the dolomite surface. Differently, in the remaining binding models, the presence of oleate on the dolomite surface did not result in an evident change in the position of  $\text{SO}_4^{2-}$ .

Our DFT calculation results essentially suggest that oleate and  $\text{SO}_4^{2-}$  anions can co-adsorb onto the defective dolomite surface. Therefore, the flotation of  $\text{H}_2\text{SO}_4$ -treated dolomite can be achieved. Meanwhile, a previous study showed that  $\text{Mg}(\text{OI})_2$  and  $\text{Ca}(\text{OI})_2$  precipitates may form on the  $\text{H}_2\text{SO}_4$ -treated dolomite surface (Zou et al., 2019). The formation of such precipitates in an aqueous system is a dynamic process that is difficult to be probed using the DFT methods with limited atoms. However, our DFT calculation results indicate that the Mg and Ca atoms on the defect sites may act as nucleation sites for the formation of  $\text{Mg}(\text{OI})_2$  and  $\text{Ca}(\text{OI})_2$  precipitates.

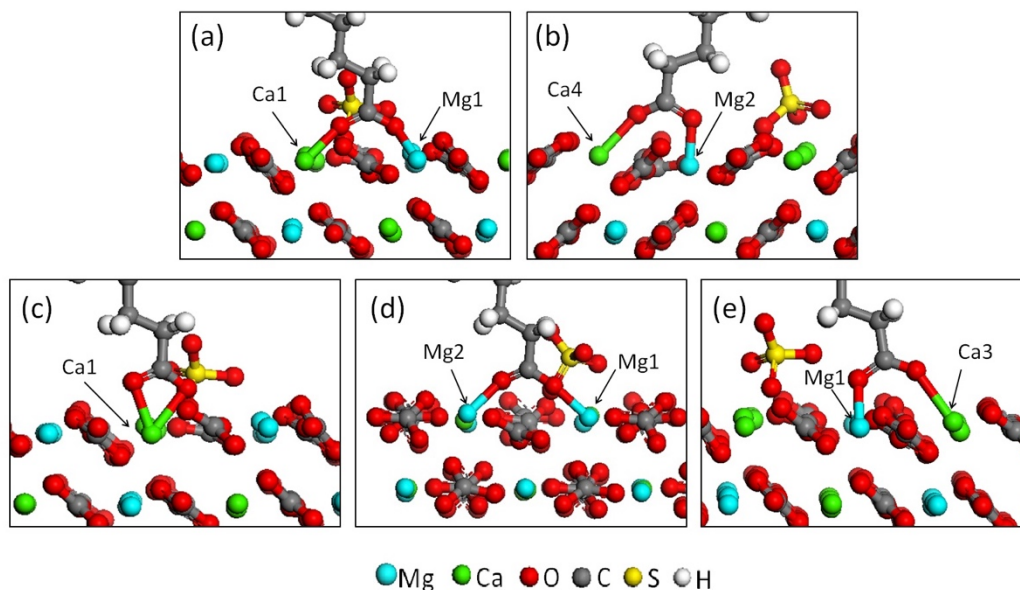


Fig. 5. Adsorption structures of oleate anion on the defective dolomite surface with  $\text{SO}_4^{2-}$  anion bonding to Ca2 atom: (a) bidentate binding to Ca1 and Mg1 (Bi1), (b) bidentate binding to Ca4 and Mg2 (Bi2), (c) Chelation binding to Ca1, (d) bidentate binding to Mg1 and Mg2 (Bi3), and (e) bidentate binding to Ca3 and Mg1 (Bi4)

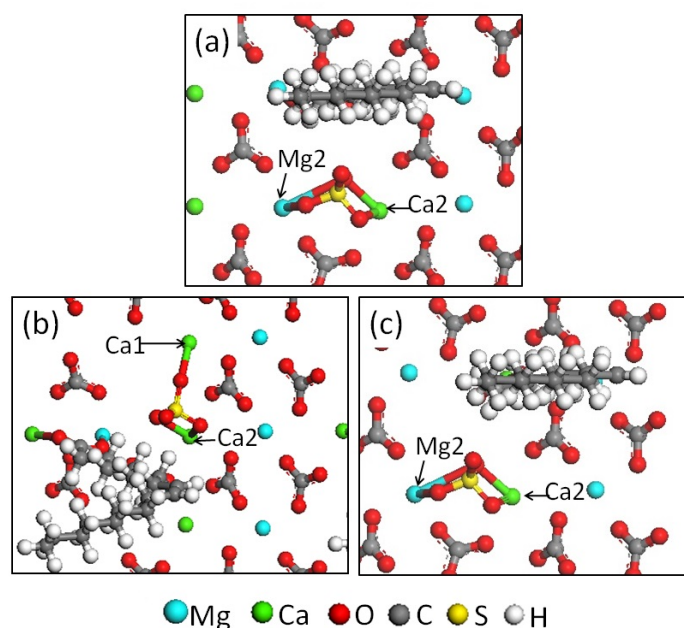


Fig. 6. Top view of the binding structures of oleate on the defective dolomite surface with  $\text{SO}_4^{2-}$  anion at the Ca2 site: (a) Bi1, (b) Bi2 and (c) Chelation binding models

### 3.3. Electron density difference analysis

Above DFT calculation results suggest that oleate and  $\text{SO}_4^{2-}$  anions can bond to the metal atoms at the defect sites on the dolomite surface. In this section, the interactions among oleate,  $\text{SO}_4^{2-}$ , and the defective dolomite surface were further evaluated via electron density difference analysis. This analysis can provide an intuitive picture of the charge redistribution arising from the interaction between bonding atoms (Cao et al., 2019). Here, we only reported the results of the Bi1 structure (Fig. 7), because this model is the most stable model for the adsorption of oleate anion on the defective dolomite surface with a  $\text{SO}_4^{2-}$  anion at the Ca2 site. The red and blue contours in the electron density difference maps refer to the charge accumulation and depletion areas, respectively.

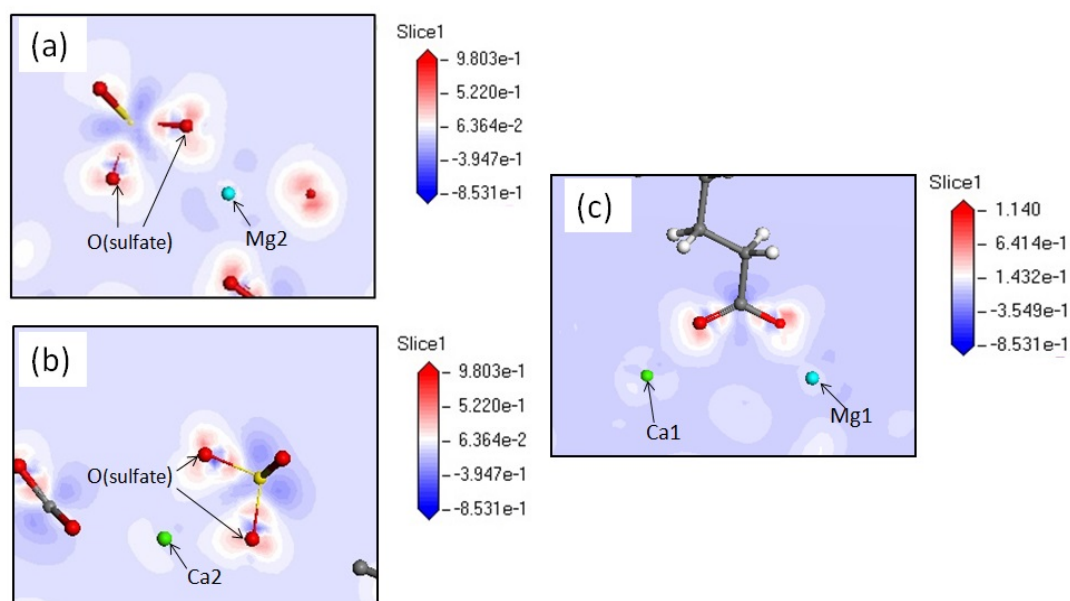


Fig. 7. Electron density difference slices of the Bi1 structure: (a) passing through two O atoms of  $\text{SO}_4^{2-}$  anion and the Mg2 atom, (b) passing through two O atoms of  $\text{SO}_4^{2-}$  anion and the Ca2 atom, and (c) passing through the two O atoms of oleate, Mg1 and Ca1 atoms

The  $\text{SO}_4^{2-}$  anion bonded with the Mg2 and Ca2 atoms on the dolomite surface in the Bi1 model. While oleate interacted with Ca1 and Mg1 in this structure, where Mg/Ca-O bonds were formed. The bonding between the O atoms in  $\text{SO}_4^{2-}$  (termed as  $\text{O}_{(\text{sulfate})}$  in Fig. 7), Ca2, and Mg2 atoms could not result in a variation in the charge density around the Ca2 or Mg2 atom. Hence, the  $\text{O}_{(\text{sulfate})}$ -Ca/Mg bond exhibited a high level of ionicity, which is consistent with the bond feature of O-Ca/Mg in dolomite crystal (F.M. Hossain et al., 2011).

A similar result was found for the bonding of oleate and the dolomite surface. The formation of O1-Mg1 and O2-Ca1 bonds scarcely changed the electron density distributions around the Mg1 and Ca1 atom. O1 and O2 are two O atoms in oleate anion (Fig. 4). The electron transfer only occurred between the atoms in oleate or  $\text{SO}_4^{2-}$ . It appears that the adsorption of oleate on such dolomite surface is primarily governed by the electrostatic attraction between oleate anion and the surface. The same results were observed in terms of the adsorption of an amino acid collector on the dolomite surface (Zou et al., 2019).

Furthermore, the electron density difference results were supported by the Mulliken charge analysis. The Mulliken charges of Ca1 and Mg1 were 1.48 e and 1.68 e, respectively, before the interaction with oleate. After the interaction, the charges of these metal atoms changed to 1.42 e and 1.74 e, respectively. Such limited variations in Mulliken charges also suggest that the O1-Mg1 and O2-Ca1 bonds are typically ionic bonds. In this regard, our electron density difference and Mulliken charge results both suggest that the electrostatic attraction force between oleate/ $\text{SO}_4^{2-}$  and metal ions on the defect dolomite surface is the major driving force for the adsorption of these species. It should be mentioned that bulk solution was not involved in this DFT study, but should be considered in future studies.

#### 4. Conclusions

The  $\text{SO}_4^{2-}$  could adsorb onto the  $\text{CO}_3$ -defect dolomite (104) surface rather than on the perfect dolomite (104) surface. Therefore, the interaction between  $\text{H}_2\text{SO}_4$  and the dolomite surface can be described in two steps: (1) two  $\text{H}^+$  ions react with a carboxyl anion, which dissociates the carboxyl anion and generates a defect site on the dolomite surface. (2) A  $\text{SO}_4^{2-}$  anion may bind with a Ca atom at the defect site. Hence,  $\text{SO}_4^{2-}$  anions could not interact with all the Ca atoms on the defective dolomite surface. Moreover, the remaining metal atoms at a defect site could react with oleate to generate five binding models, where new ionic Ca/Mg-O bonds were formed. In this regard, oleate species and sulfate anion may both occur

on the H<sub>2</sub>SO<sub>4</sub>-treated dolomite surface, which is the reason for the flotation of H<sub>2</sub>SO<sub>4</sub>-treated dolomite.

### Acknowledgments

The financial support provided by the Analysis and Testing Foundation of Kunming University of Science and Technology is gratefully acknowledged.

### References

- ARIFFIN, A.A., BAKAR, J., TAN, C.P., RAHMAN, R.A., KARIM, R., LOI, C.C., 2009. *Essential fatty acids of pitaya (dragon fruit) seed oil*. Food Chem. 114, 561-564.
- CAO, Q., ZOU, H., CHEN, X., WEN, S., 2019. *Flotation selectivity of N-hexadecanoylglycine in the fluorapatite-dolomite system*. Miner. Eng. 131, 353-362.
- CHANTURIYA, V., MASLOBOEV, V., MAKAROV, D., MAZUKHINA, S., NESTEROV, D., MENSHIKOV, Y., 2011. *Artificial geochemical barriers for additional recovery of non-ferrous metals and reduction of ecological hazard from the mining industry waste*. Environ. Lett. 46, 1579-1587.
- CHEN, Y., FENG, Q., ZHANG, G., LIU, D., LIU, R., 2018. *Effect of Sodium Pyrophosphate on the Reverse Flotation of Dolomite from Apatite*. Minerals. 8, 278.
- F.M. HOSSAIN, B.Z. DLUGOGORSHI, E.M.K., I.V. BELOVA, G.E. MURCH, 2011. *First-principles study of the electronic, optical and bonding properties in dolomite*. Comput. Mater. Sci. 50, 1037-1042.
- FRANCIS, G.P., PAYNE, M.C., 1990. *Finite basis set corrections to total energy pseudopotential calculations*. J. Phys. Condens. Matter. 2, 4395-4404.
- HORTA, D., DE MELLO MONTE, M.B., DE SALLES LEAL FILHO, E.E., 2016. *The effect of dissolution kinetics on flotation response of apatite with sodium oleate*. Int. J. Miner. Process. 146, 97-104.
- JIAO, F., WU, J., QIN, W., WANG, X., LIU, R., 2016. *Interactions of tert dodecyl mercaptan with sphalerite and effects on its flotation behavior*. Colloids Surfaces A Physicochem. Eng. Asp. 506, 104-113.
- KARLKVIST, T., PATRA, A., RAO, K.H., BORDES, R., HOLMBERG, K., 2015. *Flotation selectivity of novel alkyl dicarboxylate reagents for apatite-calcite separation*. J. Colloid Interface Sci. 445, 40-47.
- KONDRATEV, S.A., BAKSHEEVA, I.I., SEMYANOVA, D.V., 2017. *Collectability and Selectivity of Physical Adsorption of Carboxylic Acids in Flotation*. J. Min. Sci. 53, 1116-1123.
- KUSHCH, S.D., KUYUNKO, N.S., NAZAROV, R.S., TARASOV, B.P., 2011. *Hydrogen-generating compositions based on magnesium*. Int. J. Hydrogen Energy. 36, 1321-1325.
- KYLLONEN, H., PIRKONEN, P., HINTIKKA, V., PARVINEN, P., GRONROOS, A., SEKKI, H., 2004. *Ultrasonically aided mineral processing technique for remediation of soil contaminated by heavy metals*. Ultrason Sonochem. 11, 211-216.
- LIU, X., LI, C., LUO, H., CHENG, R., LIU, F., 2017a. *Selective reverse flotation of apatite from dolomite in collophanite ore using saponified gutter oil fatty acid as a collector*. Int. J. Miner. Process. 165, 20-27.
- LIU, X., LUO, H., CHENG, R., LI, C., ZHNAG, J., 2017b. *Effect of citric acid and flotation performance of combined depressant on collophanite ore*. Miner. Eng. 109, 162-168.
- LU, Y., DRELICH, J., MILLER, J.D., 1998. *Oleate adsorption at an apatite surface studied by ex-situ FTIR internal reflection spectroscopy*. J. Colloid Interface Sci. 202, 462-476.
- MATHUR, S., MOUDGIL, B.M., 1994. *Application of infrared spectroscopy in solid – solid separation processes*. Colloids Surfaces A Physicochem. Eng. Asp. 93, 137-147.
- MATIS, K.A., ZOUBOULIS, A.I., 2001. *Flotation techniques in water technology for metals recovery: The impact of speciation*. Sep Sci Technol. 36, 3777-3800.
- MICHAUX, B., RUDOLPH, M., REUTER, M.A., 2018. *Challenges in predicting the role of water chemistry in flotation through simulation with an emphasis on the influence of electrolytes*. Miner. Eng. 125, 252-264.
- PERDEW, J.P., BURKE, K., ERNERHOF, M., 1996. *Generalized gradient approximation made simple*. Phys. Rev. Lett. 77, 3865.
- PERDEW, J.P., ZUNGER, A., 1981. *Self-interaction correction to density-functional approximations for many-electron systems*. Phys. Rev. B. 23, 5048.
- PERES, A.E.C., GUIMARAES, R.C., ARAUGO, A.C., 2005. *Reagents in igneous phosphate ores flotation*. Miner. Eng. 18, 199-204.
- PRADIP, B, R., 2003. *Molecular modeling and rational design of flotation reagents*. Int. J. Miner. Process. 72, 95-110.
- PRADIP, RAI, B., RAO, T.K., KRISHNAMUTHY, S., VETRIVEL, R., MIELCZARSKI, J., CASES, J.M., 2002. *Molecular*

- Modeling of Interactions of Alkyl Hydroxamates with Calcium Minerals*. J. Colloid Interface Sci. 256, 106-113.
- QINBO, C., BIN, L., SHUMING, W., JINHUA, C., 2017. *Influence of Synergistic Effect Between Dodecylamine and Sodium Oleate on Improving the Hydrophobicity of Fluorapatite*. Physicochem. Probl. Miner. Process. 53, 42-56.
- RAI, B., P, SATHITH, PRADIP, 2008. *Molecular Modeling Based Design of Selective Depressants for Beneficiation of Dolomitic Phosphate Ores*, in XXIV International Mineral Processing Congress, (Dianzuo Wang, Chuanyao Sun, Fuliang Wang, Licheng Zhang, Long Han, Eds.), Beijing: Science Press, pp. 1518-1525.
- RAI, B., PRADIP, 2012. *Rational Design of Selective Industrial Performance Chemicals based on Molecular Modelling Computations*, CRC Press.
- RUAN, Y., HE, D., CHI, R., 2019. *Review on Beneficiation Techniques and Reagents Used for Phosphate Ores*. Minerals. 9, 253.
- SARVARAMINI, A., LARACHI, F., HART, B., 2016. *Collector attachment to lead-activated sphalerite – Experiments and DFT study on pH and solvent effects*. Appl. Surf. Sci. 367, 459-472.
- SEGALL, M., LINDAN, P.J., PROBERT, M.A., PICHARD, C., HASNIP, P., CLARK, S., PAYNE, M., 2002. *First-principles simulation: ideas, illustrations and the CASTEP code*. J. Phys. Condens. Matter. 14, 2717.
- TEMEL, H.A., 2015. *Removal of Gangue Minerals Containing Major Elements from Karlıova–Derinçay (Bingöl) Lignite Using a Reverse Flotation Method*. JOM. 67, 3002-3009.
- WAGN, X., NGUYEN, A.V., MILLER, J.D., 2006. *Selective attachment and spreading of hydroxamic acid–alcohol collector mixtures in phosphate flotation*. Int. J. Miner. Process. 78, 122-130.
- YU, J., GE, Y., GUO, X., GUO, W., 2016. *The depression effect and mechanism of NSFC on dolomite in the flotation of phosphate ore*. Sep. Purif. Technol. 161, 88-95.
- XIAOJUN, X., KELEBEK, Ş., 2000. *Activation of xanthate flotation of pyrite by ammonium salts following its depression by lime*. Dev. Miner. Process. 13, pp. C8b-43-C48b-50.
- ZOU, H., CAO, Q., LIU, D., YU, X., LAI, H., 2019. *Surface Features of Fluorapatite and Dolomite in the Reverse Flotation Process Using Sulfuric Acid as a Depressor*. Minerals. 9, 33.